Molecular and Cellular Pathobiology

Cancer Research

Truncated DNMT3B Isoform DNMT3B7 Suppresses Growth, Induces Differentiation, and Alters DNA Methylation in Human Neuroblastoma

Kelly R. Ostler[1], Qiwei Yang[2,5], Timothy J. Looney[3], Li Zhang[3], Aparna Vasanthakumar[1], Yufeng Tian[2], Masha Kocherginsky[4], Stacey L. Raimondi[1,6], Jessica G. DeMaio[1,6], Helen R. Salwen[2], Song Gu[2,7], Alexandre Chlenski[2], Arlene Naranjo[8], Amy Gill[2], Radhika Peddinti[2], Bruce T. Lahn[3], Susan L. Cohn[2], and Lucy A. Godley[1]

Abstract

Epigenetic changes in pediatric neuroblastoma may contribute to the aggressive pathophysiology of this disease, but little is known about the basis for such changes. In this study, we examined a role for the DNA methyltransferase DNMT3B, in particular, the truncated isoform DNMT3B7, which is generated frequently in cancer. To investigate if aberrant *DNMT3B* transcripts alter DNA methylation, gene expression, and phenotypic character in neuroblastoma, we measured *DNMT3B* expression in primary tumors. Higher levels of *DNMT3B7* were detected in differentiated ganglioneuroblastomas compared to undifferentiated neuroblastomas, suggesting that expression of *DNMT3B7* may induce a less aggressive clinical phenotype. To test this hypothesis, we investigated the effects of enforced *DNMT3B7* expression in neuroblastoma cells, finding a significant inhibition of cell proliferation *in vitro* and angiogenesis and tumor growth *in vivo*. DNMT3B7-positive cells had higher levels of total genomic methylation and a dramatic decrease in expression of the FOS and JUN family members that comprise AP1 transcription factors. Consistent with an established antagonistic relationship between AP1 expression and retinoic acid receptor activity, increased differentiation was seen in the *DNMT3B7*-expressing neuroblastoma cells following treatment with all-trans retinoic acid (ATRA) compared to controls. Our results indicate that *DNMT3B7* modifies the epigenome in neuroblastoma cells to induce changes in gene expression, inhibit tumor growth, and increase sensitivity to ATRA. *Cancer Res; 72(18); 4714–23. ©2012 AACR.*

Introduction

In adult cancers, epigenetic changes and aberrant splicing of *DNMT3B* are observed frequently (1, 2). Pediatric neuroblastoma is characterized by a range of clinical behaviors, and genetic and epigenetic aberrations contribute to pathogenesis (3–5). The Cohn laboratory and others have shown that hypermethylation and silencing of genes involved in the regulation of tumor growth, cell cycle, apoptosis, and DNA repair are associated with aggressive growth and poor outcome in patients (6–8). Further, poor prognosis can be predicted by a CpG island methylator phenotype (9). Preclinical studies have demonstrated that neuroblastoma growth can be inhibited by drugs that disrupt DNA methylation (10, 11). Retinoic acid, a differentiation-inducing agent that has been shown to improve clinical outcome (12), can reverse the methylation status of hundreds of gene promoters (13), possibly due to decreased levels of the DNA methyltransferase (DNMT) enzymes (14).

Three DNMT enzymes regulate DNA methylation in eukaryotic cells (15–17), with widespread aberrant *DNMT3B* transcription in cancer cells, some encoding truncated proteins lacking the catalytic domain (1, 2, 18–20). Forced expression of *DNMT3B7* within 293 cells led to altered DNA methylation levels and corresponding gene expression changes, indicating that *DNMT3B7* expression could alter DNA methylation levels and gene expression (18). *DNMT3B7* transgenic mice exhibit altered embryonic development (21).

Despite advances in genome-wide profiling that demonstrate strong correlations between genetic aberrations and clinical phenotype, we know much less about the clinical significance of epigenetic changes in neuroblastoma. Given that aberrant *DNMT3B* isoforms are common in cancer cells,

Authors' Affiliations: Departments of [1]Medicine, [2]Pediatrics, [3]Human Genetics and Howard Hughes Medical Institute, [4]Health Studies, The University of Chicago; [5]Department of Pediatrics, The University of Illinois at Chicago, Chicago, Illinois; [6]Department of Biology, Elmhurst College, Elmhurst, Illinois; [7]Department of Pediatric Surgery, Shanghai Children's Medical Center, Shanghai Jiaotong University, Shanghai, China; and [8]Children's Oncology Group (COG), University of Florida, Gainesville, Florida

Note: Supplementary data for this article are available at Cancer Research Online (http://cancerres.aacrjournals.org/).

K.R. Ostler and Q. Yang contributed equally to this work.

Corresponding Authors: Susan L. Cohn, Department of Pediatrics, The University of Chicago, KCBD-5th floor, Rm 5100, 900 E. 57th Street, Chicago, IL 60637. Phone: 773-702-2571; Fax: 773-834-1329; E-mail: scohn@peds.bsd.uchicago.edu; and Lucy A. Godley, Section of Hematology/Oncology, The University of Chicago, 5841 S, Maryland Ave., MC 2115, Chicago, IL 60637. Phone: 773-702-4140; Fax: 773-702-0963; E-mail: lgodley@medicine.bsd.uchicago.edu

doi: 10.1158/0008-5472.CAN-12-0886

we hypothesized that aberrant *DNMT3B* transcripts found in neuroblastoma tumors could alter DNA methylation, gene expression, and tumor phenotype.

Materials and Methods

Patients and tumor specimens

Two ganglioneuroblastoma, three ganglioneuroma, and fourteen primary neuroblastoma tumors were obtained from Children's Memorial Hospital in Chicago under an IRB approved protocol. Twelve RNA samples derived from one ganglioneuroblastoma and eleven neuroblastomas were obtained from the Children's Oncology Group (COG) Neuroblastoma Tumor Bank. The laboratory studies were approved by The University of Chicago Institutional Review Board.

Cell culture, cell identification, and nucleic acid isolation

Cell line identities were verified by short tandem repeat profiling using the AmpF/STR Identifiler PCR Amplification Kit (Applied Biosystems). RNA and DNA isolation was performed using TRIzol (Invitrogen) and Puregene Core Kit (Qiagen), respectively.

The MSCV-I-GFP plasmid backbone was engineered to confer constitutive *DNMT3B7* expression using a 5′ *Eco*RI site, C-terminal His-tag epitope, and 3′ *Xho*I site using primers listed in Supplementary Table S1. Retroviral constructs and packaging plasmid psi-Eco were used to produce retroviral supernatants by 293T cell cotransfection using Fugene6 Transfection Reagent (Roche).

The inducible *DNMT3B7* construct was generated using oligonucleotides listed in Supplementary Table S1 to ligate into the pRetroX-Tight-Pur response vector (pRXTPL, Clontech Laboratories). The Tet-Off System (Clontech) was used to produce inducible LA1-55n cell lines. In the presence of doxycycline, there is no induction of gene expression in either the control or *DNMT3B7*-containing cell line. In the absence of doxycycline, the *DNMT3B7*-containing cells express both *GFP* and *DNMT3B7*, and the vector control cells express only *GFP*. We have compared the vector cells expressing *GFP* to the experimental cells expressing *GFP* and *DNMT3B7* to control for any effects of *GFP* expression.

All plasmid inserts were sequenced to ensure proper correct sequence.

Neuroblastoma xenograft studies

Four- to six-week-old female homozygous athymic nude mice (Harlan) were inoculated subcutaneously into the right flank with *DNMT3B7*-expressing cells (or control) and measured twice weekly (see Supplementary Materials and Methods for details). Tumor volumes were calculated using the following formula: tumor volume = (length × width^2)/2. Mice bearing SMS-KCNR (constitutive expression) xenografts were sacrificed after 28 days. Mice bearing LA1-55n (inducible expression) xenografts were divided randomly into two groups when palpable tumors developed; control mice continued receiving doxycycline-containing water to block *DNMT3B7* expression, and animals in the experimental group were given normal drinking water to induce *DNMT3B7* expression. Mice in both groups were sacrificed after 35 days.

Immunohistochemical analysis

Immunohistochemistry was performed for CD-31 (1:100, M-20, Santa Cruz Biotechnology) to determine the mean vascular density, and Ki-67 (1:200, MIB-1, DakoCytomation) to assess proliferation rate (10).

Quantification of apoptosis

In situ detection of apoptosis was performed using the *In Situ* Cell Death Detection Kit (Roche Diagnostics Corp.; ref. 22).

Liquid chromatography/mass spectroscopy

Total cytosine methylation was performed by liquid chromatography/mass spectroscopy (LC/MS), as described previously (21).

Sodium bisulfite treatment, PCR amplification, and protein expression analysis

Genomic DNA was treated with sodium bisulfite (23), and PCR amplifications were performed using the primers listed in Supplementary Table S1 using ZymoTaq (ZymoResearch) at the indicated temperatures. Reverse transcription was performed using Superscript III (Invitrogen), and PCR amplifications were performed using Platinum Taq (Invitrogen) using primers listed in Supplementary Table S1. Whole cell extracts were made by lysing cells in 75 mmol/L NaCl, 25 mmol/L Tris-Cl, and 1:100 protease inhibitors (CalBiochem). DNMT3B was detected with T-16 antibody (1:500, sc-10236, Santa Cruz Biotechnology), and TOP1 was used as a loading control (1:400, ab3825, AbCam).

RNA-Sequencing

Total RNAs were isolated using Trizol Reagent (Invitrogen). RNA integrity was validated using the Agilent BioAnalyzer, and all samples had RNA integrity number >9. Libraries were generated following the Illumina protocol for Preparing Samples for Sequencing of mRNA. PCR amplified cDNA libraries were quantified on an Agilent 2100 Bioanalyzer. Single-end sequencing was performed for 36 cycles using Single Read Cluster Generation Kit V4 (Cat# GD-103-4001) and Sequencing Kits (Cat# FC-104-4002). Sequence reads from the RNA-sequencing (RNA-Seq) were aligned to genomic sequence (Human Feb. 2009 assembly, GRCh37/hg19). RNA-Seq data have been submitted to the GEO database, record number GSE36350.

Statistical analyses

Statistical analysis was performed using a 2-tailed Student's *t* test or Fisher' Exact Test. A P value ≤ 0.05 was considered statistically significant. For the RNA-Seq data, each DNMT3B7-expressing cell line was compared to the vector control and Bonferroni correction was used to correct for multiple testing using $n = 18{,}674$, the total number of genes that had at least one read in all 3-cell lines. Analysis of ATRA treatment of *DNMT3B7*-expressing or control cells was done using the mixed effect restricted maximum likelihood analysis model.

Results

Aberrant *DNMT3B* transcripts are expressed in primary neuroblastoma tumors

To investigate significance of aberrant *DNMT3B* transcripts in neuroblastoma, reverse transcriptase-PCR (RT-PCR) analysis was performed on a hypothesis-generating cohort of three ganglioneuroblastoma, three ganglioneuromas, and 25 primary neuroblastoma samples using primers that amplified all but 2 of the known alternative and aberrant *DNMT3B* isoforms (Fig. 1A, Supplementary Fig. S1A, Table 1). Additional *DNMT3B* transcripts were detected by Southern blot using a *DNMT3B* probe that hybridizes to all of the known aberrant isoforms amplified in the RT-PCR (Supplementary Fig. S1B and C). We stratified the patients into two risk groups: high risk and nonhigh risk. Nonhigh-risk patients included those with stages 1 and 2 disease, infants with stages 4 and 4S tumors, and patients with stage 3 tumors that lacked *MYCN* amplification. Similar to the criteria used by the COG, patients with stage 3 *MYCN*-amplified tumors and children older than 1 year of age with stage 4 disease were considered high risk (4). We found the expression of four or more aberrant *DNMT3B* isoforms correlated with higher risk groups ($P = 0.03$). The identity of *DNMT3B7* was confirmed by sequencing in four primary tumors (data not shown), and expression of *DNMT3B7* was quantified in the primary tumors by real-time RT-PCR (Supplementary Fig. S2A). We obtained ten more ganglioneuroblastoma RNAs from the COG. However, the integrity of the RNA was too low to determine the levels of *DNMT3B* isoforms (data not shown). We therefore hypothesized that high levels of *DNMT3B7* may contribute to the more benign clinical behavior of the most differentiated tumors.

Neuroblastoma cell lines showed expression patterns of *DNMT3B* transcripts similar to that of the primary tumors by RT-PCR (Fig. 1B). Tumorigenic N-type cells (24) had an increased number of *DNMT3B* transcripts and lacked *DNMT3B7*. By Western blot, we found the N-type cells have only full-length DNMT3B, whereas nontumorigenic S-type cells had both full-length DNMT3B and the truncated DNMT3B7 (Fig. 1C).

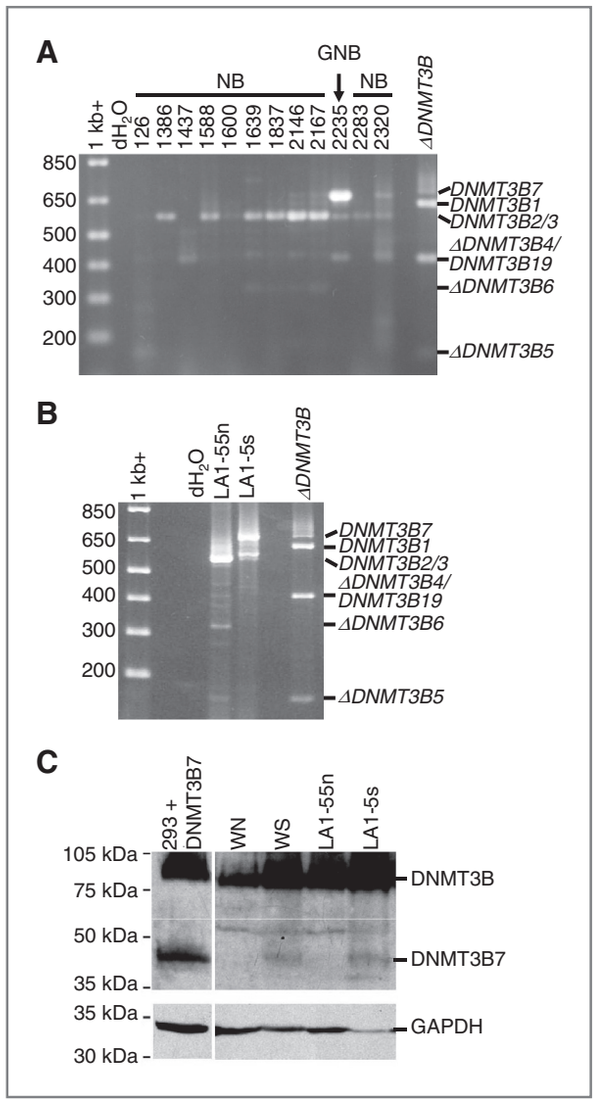

Figure 1. Aberrant DNMT3B expression and global DNA methylation in primary neuroblastoma tumors. A, RT-PCR examination of aberrant *DNMT3B* transcripts expressed in neuroblastoma (NB) and ganglioneuroblastoma (GNB) patient samples were normalized to the *GAPDH* housekeeping gene, and *DNMT3B* was amplified from exons 6 and 11 to identify the wild-type and aberrant *DNTM3B* transcripts specifically. DNA sizing is shown on the left and *DNMT3B* isoforms are shown on the right (Δ*DNMT3B*). B, RT-PCR examination of aberrant *DNMT3B* transcripts expressed in neuroblastoma cell lines, normalized to *GAPDH* housekeeping gene, and *DNMT3B* was amplified from exons 6 and 11 to specifically identify the wild-type and aberrant *DNTM3B* transcripts. DNA sizing is shown on the left, and *DNMT3B* isoforms are shown on the right (Δ*DNMT3B*). C, identification of truncated DNMT3B proteins in S-type neuroblastoma cell lines by Western blotting. The positions of the molecular weight markers are given on the left. The positions of full-length DNMT3B and truncated DNMT3B7 are indicated on the right. GAPDH was used as a loading control.

Forced expression of *DNMT3B7* in neuroblastoma cells inhibits growth

Because we detected high levels of *DNMT3B7* in differentiated tumors associated with more favorable outcomes, we hypothesized that *DNMT3B7* could modify neuroblastoma phenotype. We introduced *DNMT3B7* into an N-type neuroblastoma cell line (LA1-55n) using a Tet-off inducible system. Repression of cell growth in the *DNMT3B7*-expressing cell lines was seen after 10 days of induction ($P < 0.001$; Fig. 2A). The expression of DNMT3B7 was evaluated by Western blot analysis at each time point (Fig. 2B). DNMT3B7 expression was low during the first week and increased as the growth of the cells decreased. The level of *DNMT3B7*-expression in the induced cells was two-fold higher than what was found in ganglioneuroblastoma tumors (Supplementary Fig. S2B). Similar results were obtained using constitutive expression of *DNMT3B7* in another N-type neuroblastoma cell line, SMS-KCNR (Supplementary Fig. S3).

Both the inducible *DNMT3B7*-LA1-55n cells and constitutively-expressing *DNMT3B7*-SMS-KCNR cells were used to test the effects of *DNMT3B7* expression on tumor growth in murine xenograft models using LA1-55n cells (Fig. 3A) and SMS-KCNR

Table 1. *DNMT3B* transcripts expressed in primary ganglioneuroma, ganglioneuroblastoma, and neuroblastoma tumors

	GNB			GN			Low risk								Intermediate risk							High risk									
Tumor ID	**28**	**65–1**	**2235**	**147**	**185**	**215**	**7**	**15**	**69**	**126**	**2146**	**2167**	**2283**	**2320**	**10**	**31**	**110**	**46**	**126**	**1588**	**1600**	**48**	**57**	**113**	**114**	**246**	**280**	**1386**	**1437**	**1639**	**1837**
DNMT3B2/3	X	X	X	X	X	X	X	X	X	X	X	X	X	X	X	X	X	X	X	X	X	X	X	X	X	X	X	X		X	X
DNMT3B7	X	High	High	Faint	Faint	X	X		X		X	X		X		X		X		X		X	X	Faint	X	X					
ΔDNMT3B7		X			X				X		X	X					X	X					X			X			X	X
ΔDNMT3B6		X		X	High						X	X				X	X	X	X			X	X		X	X	X			X	X
ΔDNMT3B5										X								X	X				X	X	X	X	X	X				
Δ 3B4/3B19	X	X		X	High	X	X	X		X	X	X		X		X	X	X	X	X			X	X	X	X	X	X	X	X	X	X
Other																X			X				X									

cells (Fig. 3C). In both models, expression of *DNMT3B7* inhibited tumor growth (Fig. 3A and C). Tumor vascularity, cell proliferation, and apoptosis were evaluated in both the LA1-55n (Fig. 3B) and SMS-KCNR (Fig. 3D) xenografts with and without forced *DNMT3B7* expression. Histologic sections were stained with CD31 and showed fewer endothelial cells in the *DNMT3B7*-expressing tumors (Fig. 3B, iv and D, iv) compared to control tumors (Fig. 3B, iii and D, iii). Significantly lower mean vascular density (35.2 ± 8.3 vs 72.2 ± 9.5; $P < 0.001$) was detected in xenografts with expression of *DNMT3B7* (Supplementary Fig. S4A). In addition, blood vessels in the *DNMT3B7*-positive tumors were thin-walled and structurally more normal (Fig. 3B, ii and D, ii) than in the control tumors (Fig. 3B, i and D, i).

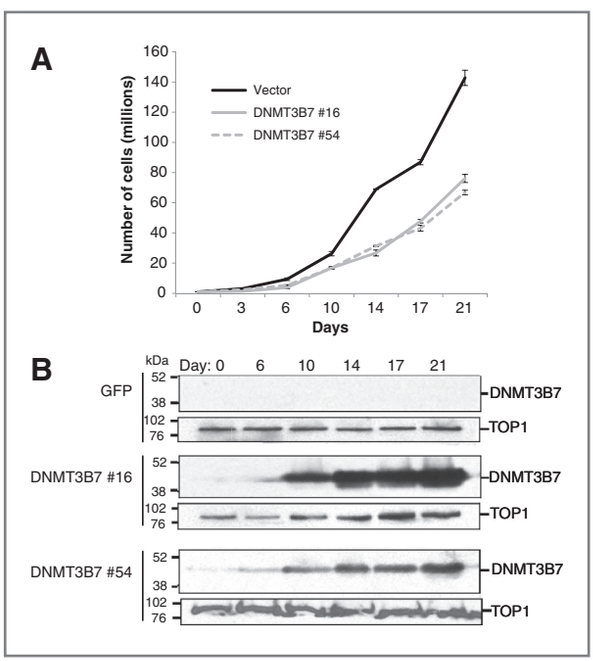

Figure 2. Establishment of neuroblastoma cells overexpressed DNMT3B7. A, LA1-55n cells were transduced with Tet-controlled transactivator and subsequently with either a Tet-off inducible *DNMT3B7* or control vector. One vector clone and two *DNMT3B7* clones were grown in the absence of doxycycline for 3 weeks to induce expression. The cells were resuspended and counted every 3 to 4 days and plated at the same density. B, whole cell extracts were made from the vector control and two *DNMT3B7*-expressing cell lines and subjected to Western blot analysis using an anti-DNMT3B antibody. Topoisomerase I was used as a loading control.

Cell proliferation in the *DNMT3B7*-positive xenografts was evaluated by Ki-67 expression, a nuclear protein that is preferentially expressed during active phases of the cell cycle. Ki-67 negative cells, representing quiescent G_0 phase cells, are more abundant in the *DNMT3B7*-expressing tumors (Fig. 3B, vi and D, vi) than in control tumors (Fig. 3B, v and D, v). Significantly higher numbers of neuroblasts in G_0 were detected in SMS-KCNR tumors with *DNMT3B7* expression, compared to control tumors (39.2 ± 3.5 vs. 14.4 ± 1.9, respectively: $P < 0.001$; Supplementary Fig. S4B). TUNEL assays demonstrated that 2.5-fold more apoptotic cells were present in the *DNMT3B7*-positive xenografts compared to controls ($P < 0.01$; Supplementary Fig. S4C). Overall, these results show that expression of *DNMT3B7* in two neuroblastoma xenograft mouse models leads to tumors with a less aggressive phenotype.

Cells with *DNMT3B7* expression have higher levels of global DNA methylation

We have shown previously that *DNMT3B7* expression in an *Eμ-Myc* transgenic mouse model resulted in an increase in global DNA methylation (21). To determine if the expression of DNMT3B7 in the LA1-55n cells also increases DNA methylation, we measured global DNA methylation levels. As shown in Fig. 4A, significantly higher levels of DNA methylation were detected in the LA1-55n cells expressing *DNMT3B7* as compared to vector control cells. We found the Satellite 2 repetitive elements had more DNA methylation following *DNMT3B7*-expression in the LA1-55n cells (Supplementary Fig S5). The increase in DNA methylation was also seen in both *DNMT3B7*-expressing xenografts. A statistically significant increase in total 5-methylcytosine levels was seen in the *DNMT3B7*-expressing xenografts compared to controls ($P < 0.01$, Fig. 4B), indicating that the pattern of DNA methylation is modified in the presence of the truncated DNMT3B7. Because we identified high levels of *DNMT3B7* in ganglioneuroblastomas, we hypothesized that this would correlate with global DNA methylation levels. We found no difference between low, intermediate, and high-risk groups. However, there was a statistically significant increase in

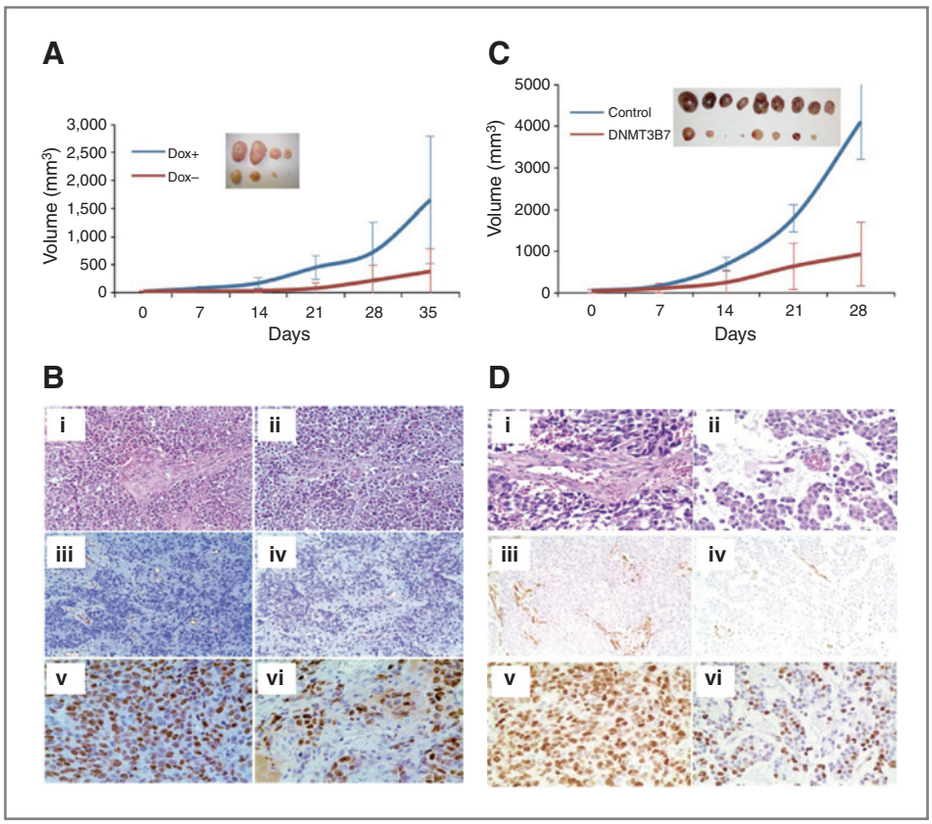

Figure 3. *In vivo* xenograft assays. A, DNMT3B7-expressing (Dox–) or control (Dox+) LA1-55n xenografts. B, H&E staining and immunohistochemistry of the LA1-55n xenograft sections. Control LA1-55n xenograft sections are on the left (i, iii, and v) and *DNMT3B7*-expressing sections on the right (ii, iv, v). H&E stained sections (i, ii). CD-31 staining (iii, iv). Ki-67 staining (v, vi). C, *DNMT3B7*-expressing or control SMS-KCNR xenografts. D, H&E staining and immunohistochemistry of the LA1-55n xenograft sections. Vector control SMS-KCNR xenograft sections are on the left (i, iii, and v) and *DNMT3B7*-expressing sections on the right (ii, iv, vi). H&E stained sections (i, ii). CD-31 staining (iii, iv). Ki-67 staining (v, vi).

global DNA methylation in the three ganglioneuroblastoma tumors (28, 65-1 and 2235), two of which have the highest level of *DNMT3B7* expression seen in any primary tumor (Fig. 4C).

DNMT3B7 expression induces changes in gene expression and DNA methylation

To investigate the effects of *DNMT3B7* on gene expression, we used RNA-Seq to compare the gene expression profiles of two independent *DNMT3B7*-expressing LA1-55n cells to vector control cells after 21 days of induction. After eliminating the genes with fewer than 150 reads per cell and those that had less than a three-fold change in either of the two *DNMT3B7*-expressing cell lines compared to the vector control, there were 144 genes that had at least an average five-fold change in the two *DNMT3B7*-expressing cell lines compared to the vector control cells (Supplementary Table S2). RNA-Seq confirmed the expression of *DNMT3B7* only in the transduced cells (Supplementary Fig. S6). Similar to the expression of *DNMT3B7* in *Eμ-Myc* transgenic mice (21), we found the expression of *DNMT1, DNMT3A* and endogenous *DNMT3B* was unchanged in the induced cells according to RNA-Seq, and real-time RT-PCR identified subtle increases in *DNMT3A* and *DNMT3B* (Supplementary Fig S7A to C). Among 117 genes with increased expression in the two *DNMT3B7*-expressing lines, 86 (73.5%) genes contained a CpG island, and 22 of the 27 (81.5%) of the genes with decreased expression contained a CpG island. Interestingly, eight of the 27 (29.6%) genes with decreased expression are found on chromosome 19 ($P = 0.0068$), and seven (25.9%) are on chromosome 19p ($P < 0.0001$). Copy number loss of chromosome 19 has been reported in 12.5% of neuroblastoma tumors (25, 26). No other chromosomal clustering of genes altered by *DNMT3B7*-expression was detected.

To identify genes that could contribute to the suppression of neuroblastoma cell growth in the presence of DNMT3B7, we focused on genes with the greatest fold changes by RNA-Seq that had CpG islands: *ANKRD12* (22-fold), *ASPM* (15-fold), and *EEA1* (14-fold; increased expression); and *FOSB* (46-fold), *ARC* (21-fold), *EGR1* (18-fold), and *FOS* (11-fold; decreased expression). In addition, we performed a GeneGo pathway analysis of all of the genes with at least a five-fold average change in expression with at least 150 reads per cell (Supplementary Table S2), which identified an additional five genes of interest: three genes that encode members of the AP1 complex that were underexpressed in the *DNMT3B7*-expressing cell lines *FOSB* (45-fold) and *FOS* (11-fold), both identified above, and *JUNB* (6-fold); genes important in neuronal function and tumorigenesis: *KIF20B* (11-fold), *ROCK1* (6-fold), *APC* (5-fold), and *RXRB* (6-fold), encoding a retinoic acid signaling coregulator that heterodimerizes with retinoic acid receptors to bind on target gene promoters at the retinoic acid response element, which is important for retinoic acid treatment of children with high-risk neuroblastoma (12). In total, we performed quantitative real-time RT-PCR of all twelve genes of interest (Fig. 5A and B).

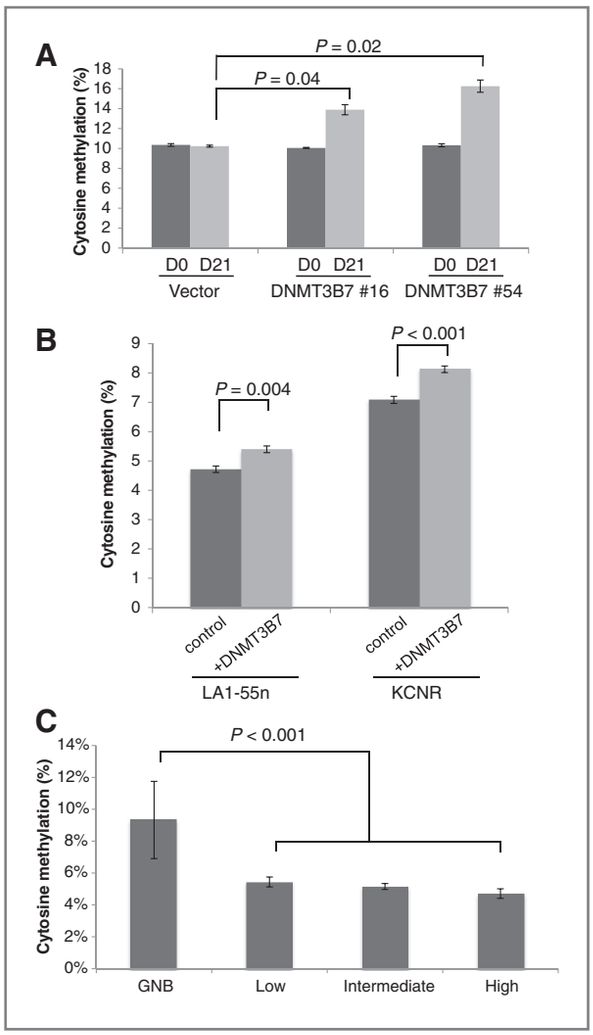

Figure 4. Global DNA methylation by LC/MS. A, global DNA methylation of a pure cell population of induced LA1-55n cells by LC/MS. B, global DNA methylation of the LA1-55n induced xenograft tumors and SMC-KCNR constitutive xenograft tumors by LC/MS. C, global DNA methylation of primary neuroblastoma tumors by LC/MS.

To test if the differential expression of genes in the *DNMT3B7*-expressing LA1-55n cells was the result of an alteration in their DNA methylation patterns, we performed bisulfite sequencing of eight genes that had been validated by real-time RT-PCR. Six of these genes showed no detectable DNA methylation across the transcriptional start site. *RXRB*, a gene important in retinoic acid signaling, showed a decrease expression of two-fold in *DNMT3B7*-expressing cells by real-time RT-PCR, and the CpG island surrounding the transcriptional start site was hypermethylated in the presence of *DNMT3B7* (Fig. 5C). Similarly, *EEA1* expression was nine-fold higher by real-time RT-PCR, and the CpG island upstream of the transcriptional start site became completely hypomethylated in *DNMT3B7*-expressing cells (Fig. 5D). The changes in DNA methylation were validated by LC/MS (Supplementary Fig. S8). These data show that expression of *DNMT3B7* in neuroblastoma cells leads changes in gene expression, some of which are correlated to altered CpG island methylation.

The effects of ATRA and *DNMT3B7* expression on growth inhibition are additive

RNA-Seq of the *DNMT3B7*-expressing LA1-55n cells revealed decreased expression of genes encoding components of the AP1 complex, *FOSB* (45-fold), *FOS* (11-fold), and *JUNB* (6-fold). In addition to acting as a transcription factor, AP1 can also antagonize the activity of retinoic acid receptors (27). We therefore hypothesized that, with reduced levels of AP1, retinoic acid receptors would be more active and could drive *DNMT3B7*-expressing cells toward differentiation. To test if retinoic acid treatment could augment the ability of DNMT3B7 to induce differentiation of neuroblastoma cells, we induced *DNMT3B7* expression in the LA1-55n cells for 2 weeks to maximize *DNMT3B7* expression (Fig. 2B). After 2 weeks of induction, both *DNMT3B7*-expressing cells and control cells were treated either with all-trans retinoic acid (ATRA) or vehicle for 7 days. We found that the effects of ATRA treatment and *DNMT3B7* expression on growth inhibition were additive (Fig. 6A), not synergistic.

To test if *DNMT3B7*-expressing cells were more differentiated than control cells, we studied the expression of 22 known neuroblastoma differentiation markers (28–33) and found that 18 of them had expression changes that correlated with a more differentiated phenotype (Supplementary Table S3). We validated the two genes with the greatest fold changes: *GFRA1* and *DLK1*. *GFRA1* encodes GDNF family receptor alpha 1 and has been shown to enhance differentiation in response to GDNF (34). *GFRA1* expression was two-fold higher in two independent *DNMT3B7*-expressing LA1-55n cell lines, compared to vector control (Fig. 6B left, dark gray bars). After ATRA treatment, *GFRA1* expression was further increased in all cell lines (Fig. 6B left, light gray bars), and this increase was greater in the *DNMT3B7*-expressing cells. *DLK1* encodes delta-like 1 homolog (*Drosophila*) and has been identified as a stem cell gene that negatively regulates differentiation (35). The expression of *DLK1* in *DNMT3B7*-expressing cells was decreased up to two-fold in two independent *DNMT3B7*-expressing LA1-55n cell lines (Fig. 6B right, dark gray bars). After ATRA treatment, *DLK1* expression was further decreased in all cell lines (Fig. 6B left, light gray bars), and the expression in the *DNMT3B7*-expressing cells was significantly lower than in the vector control cells. Taken together, these results suggest a model in which the expression of *DNMT3B7* induces neuroblastoma cells to differentiate, which can be promoted further by additional treatment by ATRA.

Discussion

DNMT3B catalyzes *de novo* methylation of DNA sequences, and high levels of this enzyme have been detected in cancer (36). In addition to full-length *DNMT3B*, more than 40 transcripts have been detected in common adult malignant tumors (18, 37). Many of the encoded proteins lack either the DNA binding or catalytic domains, and some have been shown to modify the pattern of DNA methylation and gene expression

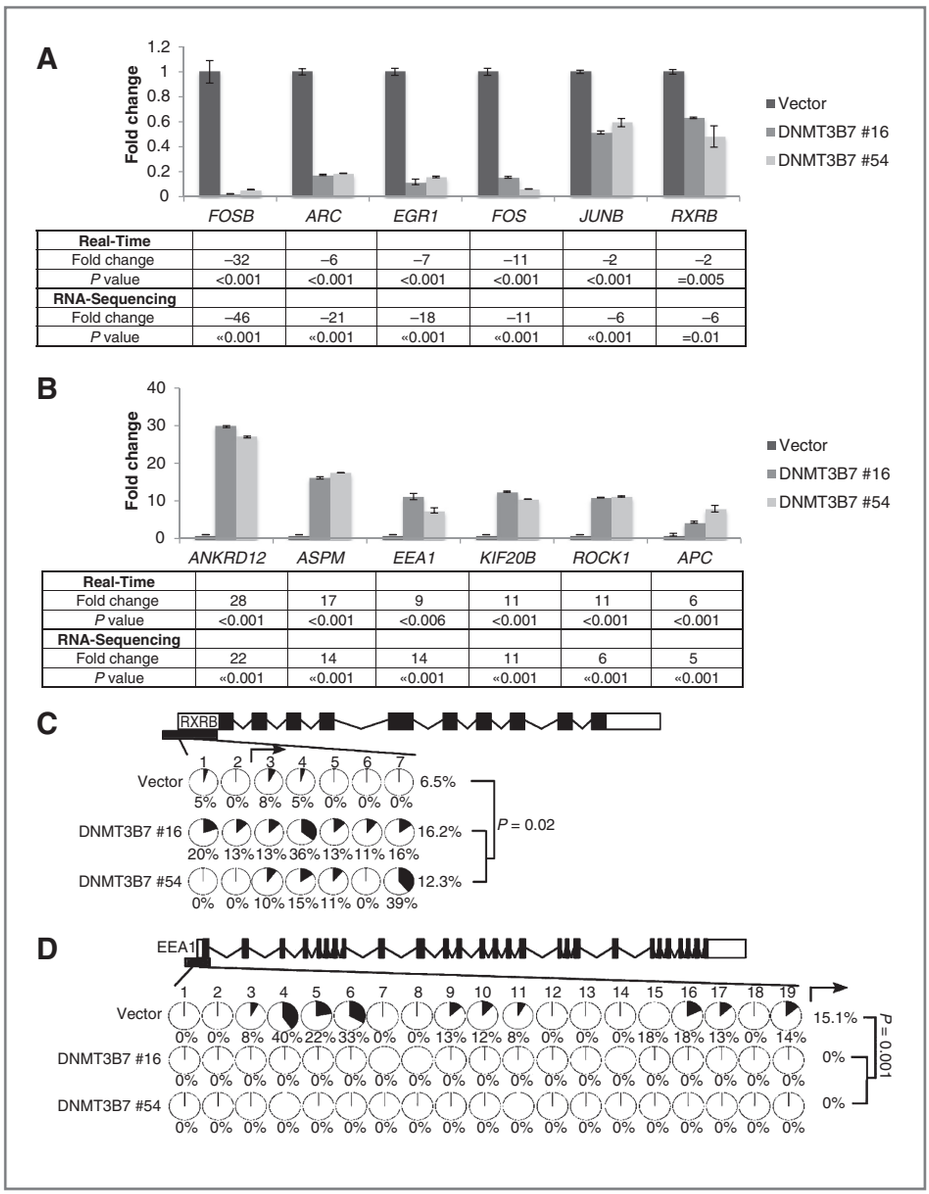

Real-Time						
Fold change	–32	–6	–7	–11	–2	–2
P value	<0.001	<0.001	<0.001	<0.001	<0.001	=0.005
RNA-Sequencing						
Fold change	–46	–21	–18	–11	–6	–6
P value	«0.001	«0.001	«0.001	«0.001	«0.001	=0.01

Real-Time						
Fold change	28	17	9	11	11	6
P value	<0.001	<0.001	<0.006	<0.001	<0.001	<0.001
RNA-Sequencing						
Fold change	22	14	14	11	6	5
P value	«0.001	«0.001	«0.001	«0.001	«0.001	«0.001

Figure 5. RNA-Seq validation and CpG island methylation. A, validation of overexpression of six genes in *DNMT3B7*-expressing cells by real-time RT-PCR. B, validation of underexpression of six genes in *DNMT3B7*-expressing cells by real-time RT-PCR. C, bisulfite sequencing of *RXRB*, a gene downregulated in *DNMT3B7*-expressing cells. D, bisulfite sequencing of *EEA1*, a gene upregulated in *DNMT3B7*-expressing cells.

(18, 20). In this study, we found *DNMT3B7* transcripts in all of the ganglioneuromas tested and at very high levels in all of the ganglioneuroblastomas, leading us to the hypothesis that *DNMT3B7* could induce differentiation and lead to a more benign phenotype, thereby modifying tumor phenotype in pediatric neuroblastoma.

To test this hypothesis, we forced *DNMT3B7* expression in neuroblastoma cells using retroviral vectors to drive either constitutive or inducible expression and evaluated its effects on DNA methylation, tumor growth, and angiogenesis. We observed growth inhibition of aggressive neuroblastoma cell lines and xenograft tumors with slowed tumor growth and suppression of angiogenesis. Although aberrant hypermethylation of specific tumor suppressor genes and a CpG-methylator phenotype have been associated with clinically aggressive neuroblastomas (37), cancer cells are globally hypomethylated compared to normal cells. Thus, the increase in global DNA methylation observed in neuroblastoma cells with forced *DNMT3B7* expression and decreased tumor growth are consistent with a non-malignant phenotype.

Previously, we have demonstrated altered DNA methylation and gene expression in 293 cells overexpressing *DNMT3B7* (18). In addition, a re-distribution of DNA methylation was observed in *DNMT3B7* transgenic mice (21). Forced expression of other DNMT3B isoforms containing the catalytic domain (ΔDNMT3B1-4) have been shown to induce hypermethylation of repetitive elements (38). The truncated DNMT3B variants that lack DNA binding or catalytic domains are likely to have altered function compared with DNMT3B, and may actually stimulate the activity

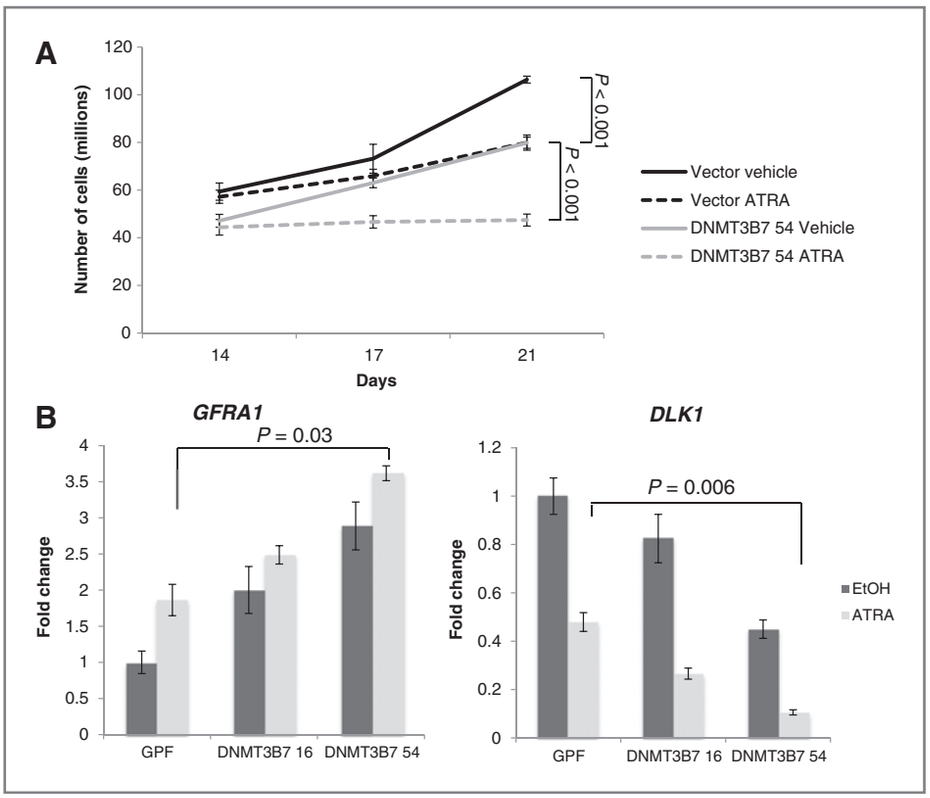

Figure 6. The effects of ATRA and DNMT3B7 expression on growth inhibition are additive. A, growth of *DNMT3B7*-expressing or control cells treated with ATRA or vehicle. Expression was induced for 2 weeks and growth in ATRA or vehicle was determined for 7 days. B, validation of increased expression of *GFRA1* and decreased expression of *DLK1*, both markers of differentiation, after treatment with ATRA or vehicle control by real-time RT-PCR.

of other DNMTs with which it heterodimerizes (39), leading to hypermethylation.

GeneGo pathway analysis of the RNA-Seq data of the *DNMT3B7*-expressing LA1-55n cells identified several genes that may be important in neuroblastoma pathogenesis: *KIF20B, ROCK1, ROCK2, APC* and genes encoding members of the AP1 complex: *FOSB*, *FOS*, and *JUNB*. Increased expression of *KIF1A* has been found to correlate with high-risk neuroblastoma tumors (40). *ROCK1* (six-fold) and *ROCK2* (six-fold) were both underexpressed in *DNMT3B7*-expressing cells, and activated RhoA and its downstream effector ROCK have been shown to be negative regulators of growth cone motility (41). Adenomatous polyposis coli (*APC*) is a tumor suppressor gene, highly expressed in the developing and adult nervous system, which is involved in neurite formation (42, 43), and apoptosis of neural crest cells (44).

Additionally, GeneGo pathway analysis of the RNA-Seq data revealed decreased expression of genes encoding the components of the AP1 complex, which can antagonize the activity of retinoic acid receptors through protein-protein interaction without requiring DNA binding (27). We therefore hypothesized that, with reduced levels of AP1, retinoic acid receptors would be more active in the *DNMT3B7*-expressing cells, allowing augmentation of differentiation by retinoid treatment. Indicative of increased differentiation, *DNMT3B7*-expressing LA1-55n cells had higher expression of *GFRA1* compared to vector controls following ATRA treatment. Similarly, the expression of *DLK1* was decreased in both *DNMT3B7*-expressing LA1-55n cell lines following ATRA treatment (Fig. 6B). It has been shown previously that ATRA treatment of another *MYCN* amplified neuroblastoma cell line (SK-N-BE) leads to promoter hypomethylation (14), although we did not observe any significant global changes in DNA methylation after ATRA treatment (Supplementary Fig. S9). In the future, screening neuroblastoma tumors for *DNMT3B7*-expression may indicate particular patients for whom ATRA treatment might be particularly effective. DNMT3B exists in a protein complex with the mitotic chromatin condensation components, including HDAC1 and SIN3A (45). When unbound, retinoic acid receptors bind NCOR2, SIN3A, and HDACs, leading to target promoter repression, which can be disassociated upon ATRA binding (46, 47).

Altered histone modifications have also been found in neuroblastoma tumors and have correlated to tumor aggressiveness. Elevated levels of EZH2, the enzymatically active component of the Polycomb Repressor Complex 2 and H3K27me3 marks have been identified at the promoters of tumor suppressors *CASZ1*, *RUNX1*, *NGFR* (*p75*), and *NTRK1* (*TrkA*) in undifferentiated, poor prognosis neuroblastoma (48). Additionally, following retinoic acid induced differentiation of neuroblastoma cells, EZH2 expression is decreased, consistent with decreased binding of EZH2 to retinoic acid inducible target genes (49). Retinoic acid treatment therefore, leads to a reduction in repressive histone marks in addition to the changes in DNA methylation described above. Therefore, future work may focus on testing whether histone modifications are altered in this system.

Our findings suggest that forced expression of *DNMT3B7* in neuroblastoma cells is able to drive genome-wide DNA methylation. This is similar to the effects seen in lymphomas that arise in *Eμ-Myc/DNMT3B7* transgenic mice (21). However, in neuroblastoma, the expression of *DNMT3B7* is anti-tumorigenic (Fig. 3), whereas *DNMT3B7* expression in *Eμ-Myc* lymphomas accelerates tumorigenesis. There are many possible explanations for this: The observations are made in different species and cell types. In addition, there are no other aberrant *DNMT3B* transcripts present in the *DNMT3B7-Eμ-Myc* lymphomas, whereas the human LA1-55n neuroblastoma cell expresses multiple *DNMT3B* transcripts. Truncated DNMT3B proteins may fine-tune the DNA methylation machinery within a cell dependent upon the other active DNMTs. These studies provide insight into understanding the molecular basis for the altered distribution of DNA methylation seen in virtually all human cancers. We hope that our discoveries will also provide a basis for novel diagnostic, prognostic, and therapeutic strategies that will be applicable to neuroblastoma and other types of tumors.

Disclosure of Potential Conflicts of Interest

No potential conflicts of interest were disclosed.

Authors' Contributions

Conception and design: K.R. Ostler, Q. Yang, S.L. Cohn, L.A. Godley
Development of methodology: K.R. Ostler, Q. Yang, L. Zhang, Y. Tian, S.L. Cohn, L.A. Godley
Acquisition of data (provided animals, acquired and managed patients, provided facilities, etc.): K.R. Ostler, L. Zhang, A. Vasanthakumar, Y. Tian, S.L. Raimondi, J.G. DeMaio, S. Gu, A. Gill, R. Peddinti, B.T. Lahn, S.L. Cohn, L.A. Godley
Analysis and interpretation of data (e.g., statistical analysis, biostatistics, computational analysis): K.R. Ostler, Q. Yang, T.J. Looney, A. Vasanthakumar, Y. Tian, M. Kocherginsky, S.L. Raimondi, H.R. Salwen, S. Gu, A. Chlenski, A. Naranjo, B.T. Lahn, S.L. Cohn, L.A. Godley
Writing, review, and/or revision of the manuscript: K.R. Ostler, Q. Yang, L. Zhang, S.L. Raimondi, J.G. DeMaio, H.R. Salwen, S. Gu, A. Chlenski, A. Naranjo, R. Peddinti, S.L. Cohn, L.A. Godley
Administrative, technical, or material support (i.e., reporting or organizing data, constructing databases): Q. Yang, L. Zhang, Y. Tian, H.R. Salwen, S.L. Cohn
Study supervision: Q. Yang, S.L. Cohn, L.A. Godley

Acknowledgments

We thank the Children's Oncology Group (COG) Neuroblastoma Biology Committee for approving this study and providing the neuroblastoma cDNA samples, and Lisa J. Guerrero and Beau Blumenschein for their contribution to this work.

Grant Support

This work was supported by funding from Children's Neuroblastoma Cancer Foundation (QY), and Comer Kids' Classic Grant (QY), NIH grants U10 CA98413 (AN), U10 CA98543 (AN), The Neuroblastoma Children's Cancer Society (SLC), Little Heroes Cancer Research Fund (SLC), Alex's Lemonade Stand (SLC), Kimmel Scholars Program (LAG), American Cancer Society grant 08-02 (LAG), and NIH CA129831 (LAG).

The costs of publication of this article were defrayed in part by the payment of page charges. This article must therefore be hereby marked *advertisement* in accordance with 18 U.S.C. Section 1734 solely to indicate this fact.

Received March 8, 2012; revised July 10, 2012; accepted July 11, 2012; published OnlineFirst July 18, 2012.

References

1. Klinck R, Bramard A, Inkel L, Dufresne-Martin G, Gervais-Bird J, Madden R, et al. Multiple alternative splicing markers for ovarian cancer. Cancer Res 2008;68:657–63.
2. Venables JP, Klinck R, Bramard A, Inkel L, Dufresne-Martin G, Koh C, et al. Identification of alternative splicing markers for breast cancer. Cancer Res 2008;68:9525–31.
3. Brodeur GM, Look AT, Shimada H, Hamilton VM, Maris JM, Hann HW, et al. Biological aspects of neuroblastomas identified by mass screening in Quebec. Med Pediatr Oncol 2001;36:157–9.
4. Maris JM, Hogarty MD, Bagatell R, Cohn SL. Neuroblastoma. Lancet 2007;369:2106–20.
5. Buckley PG, Das S, Bryan K, Watters KM, Alcock L, Koster J, et al. Genome-wide DNA methylation analysis of neuroblastic tumors reveals clinically relevant epigenetic events and large-scale epigenomic alterations localized to telomeric regions. Int J Cancer 2011;128:2296–305.
6. Teitz T, Wei T, Valentine MB, Vanin EF, Grenet J, Valentine VA, et al. Caspase 8 is deleted or silenced preferentially in childhood neuroblastomas with amplification of MYCN. Nat Med 2000;6:529–35.
7. Yang Q, Kiernan CM, Tian Y, Salwen HR, Chlenski A, Brumback BA, et al. Methylation of CASP8, DCR2, and HIN-1 in neuroblastoma is associated with poor outcome. Clin Cancer Res 2007;13:3191–7.
8. Yang Q, Zage P, Kagan D, Tian Y, Seshadri R, Salwen HR, et al. Association of epigenetic inactivation of RASSF1A with poor outcome in human neuroblastoma. Clin Cancer Res 2004;10:8493–500.
9. Issa JP. CpG island methylator phenotype in cancer. Nat Rev Cancer 2004;4:988–93.
10. Yang Q, Tian Y, Liu S, Zeine R, Chlenski A, Salwen HR, et al. Thrombospondin-1 peptide ABT-510 combined with valproic acid is an effective antiangiogenesis strategy in neuroblastoma. Cancer Res 2007;67:1716–24.
11. Yang QW, Liu S, Tian Y, Salwen HR, Chlenski A, Weinstein J, et al. Methylation-associated silencing of the thrombospondin-1 gene in human neuroblastoma. Cancer Res 2003;63:6299–310.
12. Wagner LM, Danks MK. New therapeutic targets for the treatment of high-risk neuroblastoma. J Cell Biochem 2009;107:46–57.
13. Angrisano T, Sacchetti S, Natale F, Cerrato A, Pero R, Keller S, et al. Chromatin and DNA methylation dynamics during retinoic acid-induced RET gene transcriptional activation in neuroblastoma cells. Nucleic Acids Res 2011;39:1993–2006.
14. Das S, Foley N, Bryan K, Watters KM, Bray I, Murphy DM, et al. MicroRNA mediates DNA demethylation events triggered by retinoic acid during neuroblastoma cell differentiation. Cancer Res 2010;70:7874–81.
15. Bestor TH. The DNA methyltransferases of mammals. Hum Mol Genet 2000;9:2395–402.
16. Jones PA, Baylin SB. The epigenomics of cancer. Cell 2007;128:683–92.
17. Reik W, Dean W, Walter J. Epigenetic reprogramming in mammalian development. Science 2001;293:1089–93.
18. Ostler KR, Davis EM, Payne SL, Gosalia BB, Expósito-Céspedes J, Le Beau MM, et al. Cancer cells express aberrant DNMT3B transcripts encoding truncated proteins. Oncogene 2007;26:5553–63.
19. Saito Y, Kanai Y, Sakamoto M, Saito H, Ishii H, Hirohashi S. Overexpression of a splice variant of DNA methyltransferase 3b, DNMT3b4, associated with DNA hypomethylation on pericentromeric satellite regions during human hepatocarcinogenesis. Proc Natl Acad Sci U S A 2002;99:10060–5.
20. Wang L, Wang J, Sun S, Rodriguez M, Yue P, Jang SJ, et al. A novel DNMT3B subfamily, DeltaDNMT3B, is the predominant form of DNMT3B in non-small cell lung cancer. Int J Oncol 2006;29:201–7.
21. Shah MY, Vasanthakumar A, Barnes NY, Figueroa ME, Kamp A, Hendrick C, et al. DNMT3B7, a truncated DNMT3B isoform expressed in human tumors, disrupts embryonic development and accelerates lymphomagenesis. Cancer Res 2010;70:5840–50.
22. Liu S, Tian Y, Chlenski A, Yang Q, Zage P, Salwen HR, et al. Cross-talk between Schwann cells and neuroblasts influences the biology of neuroblastoma xenografts. Am J Pathol 2005;166:891–900.

23. Clark SJ, Harrison J, Paul CL, Frommer M. High sensitivity mapping of methylated cytosines. Nucleic Acids Res 1994;22:2990–7.
24. Biedler JL, Spengler BA, Chang TD, Ross RA. Transdifferentiation of human neuroblastoma cells results in coordinate loss of neuronal and malignant properties. Prog Clin Biol Res 1988;271:265–76.
25. Chen Y, Takita J, Choi YL, Kato M, Ohira M, Sanada M, et al. Oncogenic mutations of ALK kinase in neuroblastoma. Nature 2008;455:971–4.
26. Mora J, Cheung NK, Chen L, Qin J, Gerald W. Loss of heterozygosity at 19q13.3 is associated with locally aggressive neuroblastoma. Clin Cancer Res 2001;7:1358–61.
27. Pfahl M. Nuclear receptor/AP-1 interaction. Endocr Rev 1993;14: 651–8.
28. Kaplan DR, Matsumoto K, Lucarelli E, Thiele CJ. Induction of TrkB by retinoic acid mediates biologic responsiveness to BDNF and differentiation of human neuroblastoma cells. Eukaryotic Signal Transduction Group. Neuron 1993;11:321–31.
29. Jogi A, Vallon-Christersson J, Holmquist L, Axelson H, Borg A, Pahlman S. Human neuroblastoma cells exposed to hypoxia: induction of genes associated with growth, survival, and aggressive behavior. Exp Cell Res 2004;295:469–87.
30. Hishiki T, Nimura Y, Isogai E, Kondo K, Ichimiya S, Nakamura Y, et al. Glial cell line-derived neurotrophic factor/neurturin-induced differentiation and its enhancement by retinoic acid in primary human neuroblastomas expressing c-Ret, GFR alpha-1, and GFR alpha-2. Cancer Res 1998;58:2158–65.
31. Brodeur GM, Nakagawara A, Yamashiro DJ, Ikegaki N, Liu XG, Azar CG, et al. Expression of TrkA, TrkB and TrkC in human neuroblastomas. J Neurooncol 1997;31:49–55.
32. Redfern CP, Lovat PE, Malcolm AJ, Pearson AD. Differential effects of 9-cis and all-trans retinoic acid on the induction of retinoic acid receptor-beta and cellular retinoic acid-binding protein II in human neuroblastoma cells. Biochem J 1994;304:147–54.
33. Krams M, Parwaresch R, Sipos B, Heidorn K, Harms D, Rudolph P. Expression of the c-kit receptor characterizes a subset of neuroblastomas with favorable prognosis. Oncogene 2004;23:588–95.
34. Paratcha G, Ledda F, Baars L, Coulpier M, Besset V, Anders J, et al. Released GFRalpha1 potentiates downstream signaling, neuronal survival, and differentiation via a novel mechanism of recruitment of c-Ret to lipid rafts. Neuron 2001;29:171–84.
35. Begum A, Kim Y, Lin Q, Yun Z. DLK1, delta-like 1 homolog (Drosophila), regulates tumor cell differentiation *in vivo*. Cancer Lett 318:26–33.
36. Amara K, Ziadi S, Hachana M, Soltani N, Korbi S, Trimeche M. DNA methyltransferase DNMT3b protein overexpression as a prognostic factor in patients with diffuse large B-cell lymphomas. Cancer Sci 2010;101:1722–30.
37. Abe M, Ohira M, Kaneda A, Yagi Y, Yamamoto S, Kitano Y, et al. CpG island methylator phenotype is a strong determinant of poor prognosis in neuroblastomas. Cancer Res 2005;65:828–34.
38. Choi SH, Heo K, Byun HM, An W, Lu W, Yang AS. Identification of preferential target sites for human DNA methyltransferases. Nucleic Acids Res 2011;39:104–18.
39. Van Emburgh BO, Robertson KD. Modulation of Dnmt3b function *in vitro* by interactions with Dnmt3L, Dnmt3a and Dnmt3b splice variants. Nucleic Acids Res 2011;39:4984–5002.
40. Cheung IY, Feng Y, Gerald W, Cheung NK. Exploiting gene expression profiling to identify novel minimal residual disease markers of neuroblastoma. Clin Cancer Res 2008;14:7020–7.
41. Filbin MT. Myelin-associated inhibitors of axonal regeneration in the adult mammalian CNS. Nat Rev Neurosci 2003;4:703–13.
42. Dobashi Y, Katayama K, Kawai M, Akiyama T, Kameya T. APC protein is required for initiation of neuronal differentiation in rat pheochromocytoma PC12 cells. Biochem Biophys Res Commun 2000;279: 685–91.
43. Haegele L, Ingold B, Naumann H, Tabatabai G, Ledermann B, Brandner S. Wnt signalling inhibits neural differentiation of embryonic stem cells by controlling bone morphogenetic protein expression. Mol Cell Neurosci 2003;24:696–708.
44. Hasegawa S, Sato T, Akazawa H, Okada H, Maeno A, Ito M, et al. Apoptosis in neural crest cells by functional loss of APC tumor suppressor gene. Proc Natl Acad Sci U S A 2002;99:297–302.
45. Geiman TM, Sankpal UT, Robertson AK, Chen Y, Mazumdar M, Heale JT, et al. Isolation and characterization of a novel DNA methyltransferase complex linking DNMT3B with components of the mitotic chromosome condensation machinery. Nucleic Acids Res 2004;32:2716–29.
46. Chen JD, Evans RM. A transcriptional co-repressor that interacts with nuclear hormone receptors. Nature 1995;377:454–7.
47. Heinzel T, Lavinsky RM, Mullen TM, Söderstrom M, Laherty CD, Torchia J, et al. A complex containing N-CoR, mSin3 and histone deacetylase mediates transcriptional repression. Nature 1997;387:43–8.
48. Wang C, Liu Z, Woo CW, Li Z, Wang L, Wei JS, et al. EZH2 Mediates epigenetic silencing of neuroblastoma suppressor genes CASZ1, CLU, RUNX3, and NGFR. Cancer Res 2011;72:315–24.
49. Lee ER, Murdoch FE, Fritsch MK. High histone acetylation and decreased polycomb repressive complex 2 member levels regulate gene specific transcriptional changes during early embryonic stem cell differentiation induced by retinoic acid. Stem Cells 2007;25:2191–9.